Supporting Information

Analysis of the X-ray powder diffraction data proceeded in the usual sequence of steps:

1. Data Collection
2. Indexing the Pattern
3. Extraction of the Peak Intensities
4. Structure Determination
5. Rietveld Refinement

The results are reported in the main manuscript. Further information regarding the details of the analysis and choices made along the way are given in the material that follows.

1. Data Collection

X-ray powder diffraction data were collected on fresh samples of $[(^tBuCO_2)_3Mo_2(\mu\text{-}O_2CC_6F_4CO_2)Mo_2(O_2C^tBu)_3]$ (Mo_4PFT) and the tungsten analogue (W_4PFT), using an in-house Bruker D8 diffractometer. This system is equipped with a Cu X-ray tube, an incident beam Ge monochromator, a spinning capillary stage, and a scintillation detector. Due to the air-sensitive nature of these compounds the samples were sealed in ~0.7 mm diameter capillaries, inside a glove box prior to data collection. The Mo_4PFT and W_4PFT diffraction patterns were very similar in both the positions and intensities of the peaks, suggesting that these two compounds are isostructural. Unfortunately, the XRD pattern of the tungsten compound was not of sufficient quality to warrant further analysis.

2. Indexing the Pattern

The positions of the first 18 peaks diffraction patterns were determined using the peak fitting routine in the CMPR software package.[1] The peak positions were then input to the CRYSFIRE autoindexing package.[2] Indexing runs using both DICVOL[3] and TREOR[4], identified a single unit cell that could account for all of the observed peaks. The unit cell was monoclinic with dimensions a = 21.02 Å, b = 5.72 Å, c = 20.55 Å and β = 101.4°, with a figure of merit[10] F_{18} equal to 34. The systematic absences were consistent with a C-centered unit cell. Further absences, such as those that arise from the presence of an axial glide plane, were not consistent with the data. Thus we were able to narrow the list of possible space groups down to three: *C2*, *Cm* and *C2/m*.

3. Extraction of the Peak Intensities

Peak intensities were extracted using the whole pattern fitting routine in DASH,[5,6] which is based on the Pawley method,[7] The patterns were also fit using a whole pattern approach based upon the LeBail method[8] as implemented in the GSAS software suite.[9] Since the three space groups that emerged from the indexing stage (*C2, Cm* and *C2/m*) have identical systematic absences so that they all give identical fits to the data at the whole pattern fitting stage. Peak extraction using DASH (Pawley method) gave a profile χ^2 value of 2.52. Peak extraction using GSAS (LeBail method) gave a χ^2 value of 1.62 and a R_{wp} value of 0.0556. The LeBail fit to the Mo_4PFT laboratory XRD pattern is shown in Figure S1.

Figure S1: LeBail fit to the laboratory X-ray powder diffraction data for $[(^tBuCO_2)_3Mo_2(\mu\text{-}O_2CC_6F_4CO_2)Mo_2(O_2C^tBu)_3]$. Blue points represent the experimental diffraction pattern, the green line represents the refined fit to the pattern, the red line represents the difference curve, and the black ticks mark the expected peak positions.

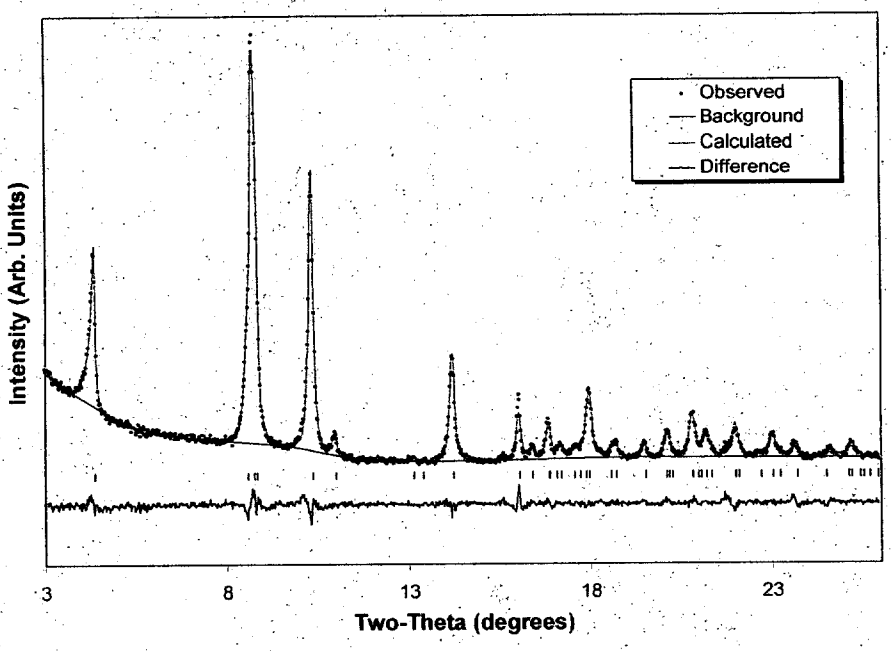

Figure S2: Rietveld fit to the laboratory X-ray powder diffraction data, using the *C2* solution for $[(^tBuCO_2)_3Mo_2(\mu\text{-}O_2CC_6F_4CO_2)Mo_2(O_2C^tBu)_3]$ as obtained from DASH. Blue points represent the experimental diffraction pattern, the green line represents the refined fit the the pattern, the red line represents the difference curve, and the black ticks mark the expected peak positions.

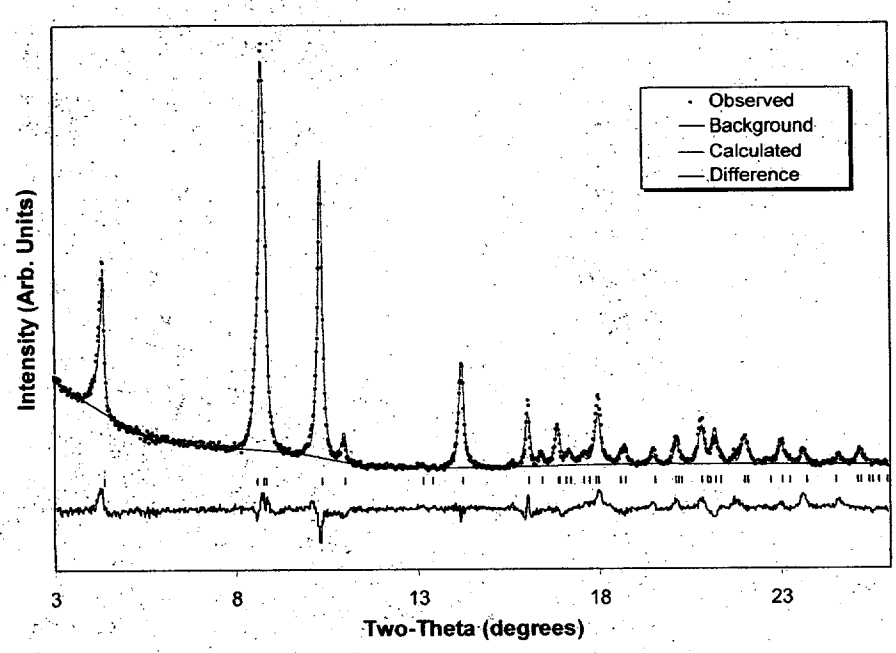

4. Structure Determination

Following the autoindexing and whole pattern fitting stages each of the three possible space groups was further investigated at the structure solution stage described below. The molecular geometry was determined using density functional theory calculations as described in the main body of the paper. The structure determination was carried out using the global optimization approach implemented within DASH, the details of which are described elsewhere.[6]

In the absence of special constraints associated with space group symmetry, the optimization process looks to obtain the best match to the experimental data by adjusting the following variables:

- 3 variables to describe the position of the molecule within the unit cell,
- 4 variables (quaternians[11]) to describe the orientation of the molecule,
- 6 torsional degrees of freedom associated with the *tert*-butyl group on each pivalate ligand,
- 2 torsional degrees of freedom associated with twists about the C-C bond of each carboxylate group extending from the phenyl ring.

This reduces the number of variables from 186 (3 variables each for the 62 crystallographically distinct non-hydrogen atoms) to 15. However, the restraints imposed by the space group symmetry are not insignificant in this case. Regardless of the choice of space group, the conformation of the molecule is no longer independent of symmetry. That is to say that not all atoms in the Mo_4PFT molecule are crystallographically unique ($Z' < 1$).

C2 → The two-fold axis must intersect the center of gravity of the molecule (the center of the aromatic ring), so that the two halves of the molecule are related by symmetry ($Z' = ½$). Since the y-coordinate of the molecule's position is arbitrary, there are no variables associated with the position of the molecule. By symmetry the aromatic ring should lie either parallel or perpendicular to the two fold axis so that only 1 variable is needed to specify the orientation of the molecule (a rotation about the *b*-axis). Finally, as the left hand side of the molecule is related to the right-hand side by symmetry there are only four torsional degrees of freedom. (5 variables)

Cm → As the *b*-axis is only one molecule wide (along the shortest dimension of the molecule where no pivalate groups are extending out from the Mo-Mo multiple bond), the mirror plane must bisect the molecule. Thus the y-coordinate of the molecule is fixed, and its position in the xz-plane is arbitrary. This configuration also constrains the perfluoroterephthalate group (save the four oxygens), and three carbons from each pivalate group to lie on the mirror plane (molecular symmetry is C_{2h}). This leaves one variable to define the orientation of the molecule (a rotation about the *b*-axis) and two torsional degrees of freedom associated with the *tert*-butyl groups. (3 variables)

C2/m → This space group combines the symmetry constraints of *C2* and *Cm*. The resulting rigid body refinement involves only one variable, which defines the orientation of the molecule. (1 variable)

As $Z' < 1$ for each of the above space groups, the structure optimization process for Mo_4PFT represents a somewhat non-standard application of DASH. In order to be strictly correct one should use a molecular fragment during the optimization process. However, in practice it was difficult to constrain the position of the molecular fragment to be in the proper location with

respect to the respective symmetry operators. Therefore, the entire molecular was used during the optimization process. A correct solution can still be obtained if the molecule moves to a conformation where the symmetry operators map the molecule onto itself. In this case the overall scale factor can be varied to obtain appropriate occupancies. This was the behavior observed when the space group symmetry was taken to be *C2*, with the exception of 4 carbon and 4 fluorine atoms of the bridging perfluoroterephthalate group. The failure of these atoms to map onto each other is discussed in the next section. The DASH profile χ^2 for the *C2* solution was a very respectable 5.82. As discussed above, when the space group symmetry was taken to be either *Cm* or *C2/m*, the torsion angles and molecular orientation had to be fixed so that the mirror plane bisects the Mo-Mo bond and contains the aromatic ring. Those constraints lead to a very unsatisfactory fit to the data, yielding a profile χ^2 value of 84. Thus we can unambiguously discard the *Cm* and *C2/m* solutions and confirm that *C2* is the appropriate space group symmetry.

5. Rietveld Refinement

As a final step in the structure determination process a rigid body Rietveld refinement was performed using the GSAS software suite,[9] with the initial position and orientation of the molecules being taken from the DASH output. A rigid body refinement was attempted and found to be stable, but did not lead to a noticeable improvement in the fit. Therefore, the atomic positions obtained from DASH were not refined. The background was modeled using a linear interpolation between manually selected, fixed background points. The variables that were refined included the lattice parameters, a zero-point shift, peak shape parameters, a scale factor and a single isotropic displacement parameter.

Attempts were made to improve the fits by removing the rigid body constraints. These refinements were only stable if a large number of soft constraints were placed on the Mo-Mo, Mo-O, C-O, C-C, C-F and O-O distances, and these constraints were weighted very heavily. While this did lead to an improvement in the fit to the experimental pattern, it was not clear that a more accurate picture of the molecular conformation and packing was obtained. Undoubtedly, some distortions of the calculated gas phase molecular geometries are present in the solid-state structure, but much better diffraction data would be needed in order to reliably extract this information.

As discussed at length in the previous section, the center of mass of the Mo_4PFT molecule lies on a 2-fold rotation axis so that the two halves of the molecule are related by symmetry ($Z' = ½$). Within the constraints of symmetry there are two possible ordered orientations of the planar aromatic ring, either parallel or perpendicular to the 2-fold axis. Alternatively, the plane of the $O_2CC_6F_4CO_2$ group could be disordered over two or more orientations. All three possibilities were evaluated during the final refinement stage. The disordered model provided a fit ($R_{wp} = 0.0796$) to the experimental data far superior to models with the PFT group either parallel ($R_{wp} = 0.142$) or perpendicular ($R_{wp} = 0.113$) to the 2-fold axis. Additionally, the model with the aromatic ring parallel to the 2-fold axis leads to unrealistically short (~ 1 Å) F-F contacts. The final refinement results are contained in Tables S1 and S2, and the final fit to the data is shown in Figure S2.

One can understand the disorder of the aromatic ring through inspection of Figures 2 and 3 of the main paper. The strongest intermolecular interactions exist along the *b*-axis, which suggests that all molecules in the one dimensional polymeric chains adopt the same orientation of the C_6F_4 ring, as shown in figures 2 and 3. Furthermore, the crystal packing would significantly disturbed along the c-direction (vertical direction in Figure 2) if the orientation of

the aromatic ring were randomized. In contrast, along the a-direction (horizontal direction in Figure 2) the intermolecular interactions are largely van der Waals interactions between pivalate groups, so that the bridging PFT groups play almost no role. One can easily imagine that a reversed orientation of the aromatic ring alignment in a chain neighboring along *a* would do little to destabilize the molecular packing.

Table S1: Crystallographic data for $[(^tBuCO_2)_3Mo_2(\mu\text{-}O_2CC_6F_4CO_2)Mo_2(O_2C^tBu)_3]$

Temperature/K	295
Formula Weight/g mol^{-1}	1226
Space Group	*C2*
a/Å	21.011(3)
b/Å	5.7245(8)
c/Å	20.586(3)
β/°	101.307(7)
Volume/$Å^3$	2427.8(7)
Z	2
Calculated Density/g cm^{-3}	1.68
LeBail R_{wp} (Lab Data)	0.0556
Rietveld R_{wp} (Lab Data)	0.0796

Table S2: Fractional coordinates for $[(^tBuCO_2)_3Mo_2(\mu\text{-}O_2CC_6F_4CO_2)Mo_2(O_2C^tBu)_3]$

Atom	x	y	z	Occupancy
Mo1	0.6253	0.9503	0.2817	1
Mo2	0.5825	0.6206	0.2541	1
C1	0.4739	0.7680	0.5582	1
C2	0.5207	0.6057	0.5487	0.5
C3	0.5464	0.6091	0.4913	0.5
C5	0.4791	0.9372	0.4515	0.5
C6	0.4534	0.9338	0.5090	0.5
C7	0.4463	0.7643	0.6200	1
C8	0.6541	0.7922	0.1558	1
C9	0.6824	0.7962	0.0927	1
C10	0.7128	0.5693	0.3342	1
C11	0.7739	0.4476	0.3718	1
C12	0.4946	1.0017	0.2024	1
C13	0.4331	0.1232	0.1659	1
C14	0.4298	0.3694	0.1932	1
C15	0.3729	-0.0137	0.1748	1
C16	0.4331	0.1365	0.0917	1
C17	0.6405	0.6465	0.0397	1
C18	0.7518	0.7014	0.1069	1
C19	0.6845	0.0465	0.0671	1
C20	0.7552	0.2689	0.4195	1
C21	0.8205	0.6265	0.4107	1

C22	0.8093	0.3246	0.3232	1
F1	0.4084	1.0918	0.5169	0.5
F2	0.5413	0.4443	0.5954	0.5
F3	0.5914	0.4511	0.4834	0.5
F4	0.4585	1.0986	0.4049	0.5
O1	0.5873	0.9544	0.3699	1
O2	0.5422	0.6060	0.3407	1
O3	0.6656	0.9652	0.1952	1
O4	0.6204	0.6164	0.1660	1
O5	0.7114	0.7915	0.3341	1
O6	0.6661	0.4426	0.3048	1
O7	0.4962	0.7794	0.2022	1
O8	0.5415	0.1285	0.2314	1

References

1. CMPR was written by Brian Toby. Academic users can obtain this software free of charge at http://www.ncnr.nist.gov/programs/crystallography/software/cmpr/.
2. CRYSFIRE was written by Robin Shirley. Academic users can obtain this software free of charge at http://www.ccp14.ac.uk/tutorial/tutorial.htm.
3. A. Boultif and D. Louer, *J. Appl. Crystallogr.*, 1991, **24**, 987.
4. P. E. Werner, L. Eriksson and M. Westdahl, *J. Appl. Crystallogr.*, 1985, **18**, 367.
5. DASH was written by W.I.F. David and K. Shankland, and can be purchased from the Cambridge Crystallographic Data Centre, see www.ccdc.cam.ac.uk for more details.
6. W. I. F. David, K. Shankland and N. Shankland, *Chem. Commun.*, 1998, 931.
7. G. S. Pawley, *J. Appl. Crystallogr.*, 1981, **14**, 357.
8. A. LeBail, H. Duroy and J. L. Fourquet, *Mater. Res. Bull.*, 1988, **23**, 447.
9. A. C. Larson and R. B. Von Dreele, 'GSAS Software Suite', Los Alamos, NM.
10. G. S. Smith and R. L. Snyder, *J. Appl. Crystallogr.*, 1979, **12**, 60.
11. A. R. Leach, 'Molecular Modeling: Principles and Applications', 1996.

Figure S3: Excitation profiles of the key bands of W_4PFT at 313, 518 and 1288 cm^{-1}, respectively, along with the electronic spectrum of the complex recorded as a Nujol™ mull at *ca* 80 K.

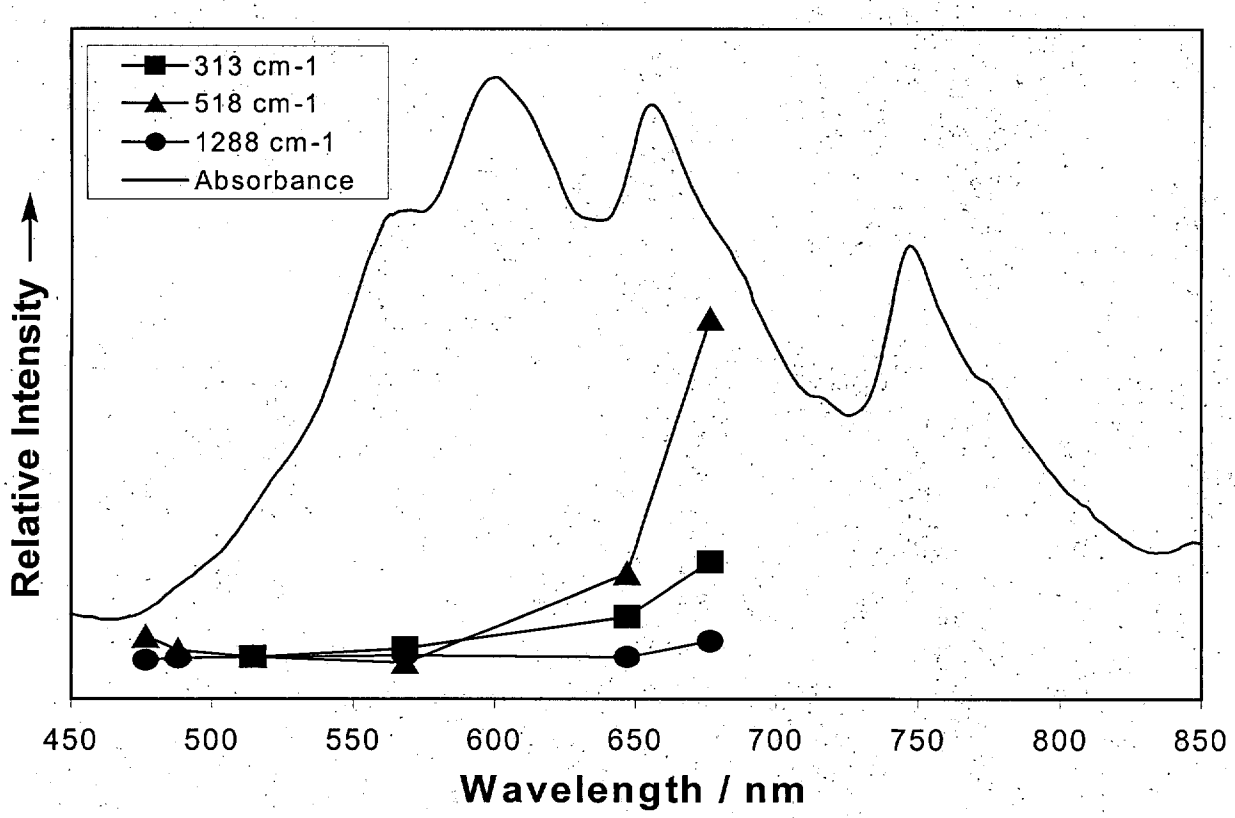

Figure S4: Excitation profiles of the key bands of Mo_4PFT at 399, 436 and 518 cm^{-1}, respectively, along with the electronic spectrum of the complex in tetrahydrofuran solution at 300 K.